Bull. Mater. Sci., Vol. 35, No. 2, April 2012, pp. 233–242. © Indian Academy of Sciences.

Study on crystallization behaviour of co-polyamide 66 containing triaryl phosphine oxide

YANG XIAO FENG*, LI QIAO LING, CHEN ZHI PING, YANG YONG FENG and ZHANG LEI
Department of Chemistry, School of Science, North University of China, Taiyuan 030051, China

MS received 2 December 2010; revised 3 April 2011

Abstract. In this paper, the isothermal crystallization and non-isothermal crystallization behaviour of flame retardant co-polyamide 66 (FR-PA66) containing triaryl phosphine oxide (TPO) were researched by employing differential scanning calorimetry (DSC), polarized optical microscopy (POM), respectively. The effects of TPO groups on nucleation mechanism, nucleation pattern and crystallization rate of FR-PA66 were discussed in detail. Experimental results show that TPO unit does not nucleate first during crystallization process of FR-PA66. The nucleation mechanism and nucleation pattern of FR-PA66 do not virtually change with incorporation of TPO groups when compared with polyamide 66 (PA66). The mainly crystallization process of FR-PA66 is still free nucleation and growing during the prime crystallization stage, and is unimensional nucleation and growing during the second crystallization stage. But at the second crystallization stage, we think there is a para-crystal forming with the main-crystal unimensional nucleation and growing. In addition, incorporation of TPO groups result in the decrement of both nucleation rate and crystallization rate of FR-PA66, and the increment of crystallization activation energy. Hence the TPO groups were unfavourable for FR-PA66 crystallization. In addition, incorporation of TPO groups also result in the decrement of crystallization region of FR-PA66, and increment of spherulite defect.

Keywords. Triaryl phosphine oxide; co-polyamide 66; crystallization behaviour; nucleation mechanism.

1. Introduction

Triaryl phosphine oxide (TPO) compounds, which as a type of flame retardant containing phosphine, play an important role in polymer flame retardant field. In our previous research (Xiaofeng Yang *et al* 2009), a typical TPO compound, [bis(4-carboxyphenyl)phenyl phosphine oxide (BCPPO)] used as a raw material and was introduced into polyamide 66 (PA66) through two-step *in-situ* polymerization reaction. And intrinsic flame retardant polyamide 66 (FR-PA66) containing TPO were fabricated. Further research indicated that FR-PA66 demonstrates excellent mechanical and flame retardant properties. In this work, the effects of TPO unit on crystallization behaviour of FR-PA66 such as crystallization process, crystallization kinetic, crystallization rate and crystallization mechanism were deeply discussed. And crystallization kinetic parameters were calculated. This research establish the fundamental for further getting a clear understanding of polymer crystallization process and crystallization mechanism, and provide the fundamental data for processing and application of FR-PA66.

*Author for correspondence (yang57705@sina.com)

2. Experiment and data processing methods

2.1 *Materials and testing measurements*

2.1a *Materials*: In this work FR-PA66 was fabricated according to the literature (Xiaofeng Yang *et al* 2009) by two *in-situ* polymerization reactions with BCPPO as raw material. The structure of FR-PA66 is shown in figure 1.

2.1b *Differential scanning calorimetry (DSC) testing*: Isothermal, non-isothermal crystallizations and subsequent melting behaviours of FR-PA66 were carried out using a STA449C, and the temperature was calibrated with the indium standard. All DSC experiments were performed under a nitrogen purge with a constant flow rate. Sample weights were between 2 and 3 mg. All samples were dried at 120°C under vacuum for 12 h before measurement. DSC experiments of isothermal crystallization and subsequent melting behaviours were performed as follows: the sample was heated to 300°C at a rate of 50°C/min and held at this temperature for 10 min to eliminate any previous thermal history, and then cooled at a rate of −100°C/min to the predetermined cryatallization temperature (T_c), ranged from 210 to 218°C in steps of 2°C and was maintained at T_c for 1 h necessary for the DSC trace to return to the calorimeter baseline. The specimens were subsequently heated to 300°C at a rate of 50°C/min. DSC measurements of non-isothermal crystallization were performed following the similar process described above. All samples were heated to 300°C at a rate

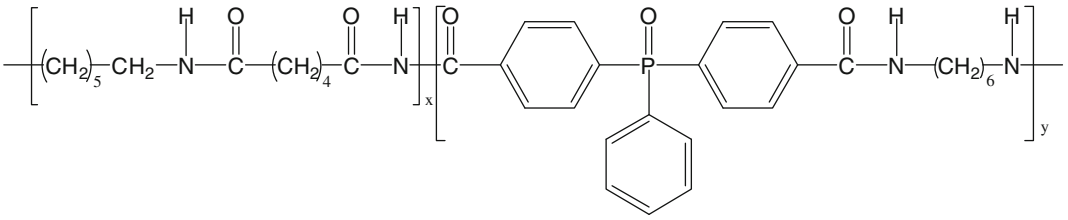

Figure 1. Structure of FR-PA66.

of 10°C/min every time and then DSC cooling traces were recorded at the rates of 2·5, 5, 10, 20 and 40°C/min.

2.1c *Polarized optical microscopy (POM) testing*: POM testing was performed as follows: a small film of FR-PA66 was cut and fixed between microslide and deckglass, then the sample was heated to 240°C under a nitrogen purge. A vertical slight stress was exerted to deckglass after melting. The sample was maintained at 240°C for 4·5 h to form crystallization, subsequently cooled to room temperature. The image of spherulite growing of FR-PA66 was observed with POM.

In order to compare the difference of crystallization process and crystallization state after and before TPO unit incorporation into FR-PA66, above testing measurements were also carried out with PA66.

2.2 *Data process methods*

In this research, the data of isothermal crystallization were processed and plotted with Avrami equation according to the literature (Avrami 1939, 1940, 1941). And the data of non-isothermal crystallization were processed and plotted with Avrami-Jeziorny (Jeziorny 1978) and Mo's equation (Liu Jieping and Mo Zhishen 1991; Gao Huan and Mo Zhishen 1992; Liu *et al* 1997), respectively.

2.2a *Avrami equation*: Avrami equation is widely used in the research of polymer isothermal crystallization kinetic. And its common form is as follows:

$$X(t) = 1 - \exp(-Kt^n),$$

or

$$\lg\{-\ln[1 - X(t)]\} = n \lg t + \lg K. \tag{1}$$

Here K is crystallization rate constant and n Avrami exponent, which have relationships with nucleation mechanism and nucleation pattern during polymer crystallization. The value of n is the sum of space and time dimension in crystallization. $X(t)$, as a function of time, is relative degree of crystallinity and is calculated with the following equation.

$$X(t) = \frac{X_c(t)}{X_c(t=\infty)} = \frac{\int_0^t \frac{dH_c(t)}{dt} dt}{\int_0^{t=\infty} \frac{dH_c(t)}{dt} dt},$$

where $X_c(t)$ and $X_c(t = \infty)$ are relative crystallinity degree of polymer when crystal time is t and final respectively. $dH_c(t)/dt$ is rate of heat flow when crystal time is t, and is calculated by DSC curves of isothermal crystallization.

When $\lg\{-\ln[1-X(t)]\}$ vs $\lg t$ were plotted, we can get Avrami exponent n and crystallization rate constant K by the slope and intercept of straight line.

2.2b *Avrami–Jeziorny equation*: Avrami–Jeziorny equation is used to research the non-isothermal crystallization kinetic of polymer. And its form is as follows:

$$\lg\{-\ln[1 - X(t)]\} = n \lg t + \Phi \lg Z_c. \tag{2}$$

Here Φ is the cooling rate and Z_c is complex crystallization rate constant. When plot $\lg\{-\ln[1-X(t)]\}$ vs $\lg t$, we can also get Avrami exponent n and complex crystallization rate constant Z_c by the slope and intercept of straight line.

2.2c *Mo's equation*: By combined Avrami and Ozawa models (Ozawa 1971), Mo *et al* (Liu Jieping and Mo Zhishen 1991; Gao Huan and Mo Zhishen 1992; Liu *et al* 1997) suggested a novel kinetic approach, named Mo's model, for analysis of non-isothermal crystallization kinetic of polymer. The form of Mo's equation is as follows:

$$\lg \Phi = \frac{1}{m} \lg \frac{K_T}{K} - \frac{n}{m} \lg t.$$

Here m is Ozawa exponent, which also have relationship with growing dimension of crystal; K_T is crystallization rate constant. Assuming that $F(T) = [K(T)/K]^{\frac{1}{m}}$, and $a = \frac{n}{m}$, the parameter $F(T)$ has a definite physical and practical meaning and is the value of cooling rate which has to be chosen at a unit crystallization time when the measured system amounts to a certain degree of crystallinity, the parameter a is the ratio of the Avrami exponent, n, to the Ozawa exponent, m. The final form was obtained as follows:

$$\lg \Phi = \lg F(T) - a \lg t. \tag{3}$$

3. Results and discussion

3.1 *Effects of TPO on equilibrium melting temperature and crystallization properties*

Figure 2 presents the DSC heating curves of FR-PA66 and virgin PA66 after completion of isothermal crystallization at various crystallization temperatures, respectively. From

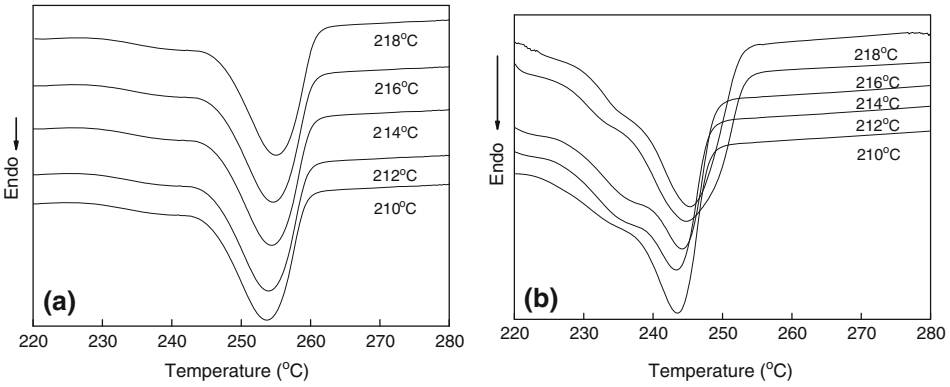

Figure 2. Melting curves of (**a**) PA66 and (**b**) FR-PA66 after isothermal crystallization at various temperatures.

DSC heating curves, we found that there is a main melting endotherm peak for all samples of both PA66 and FR-PA66, near 255°C and 245°C, respectively. The main endotherm peaks were contributed to the melting of main-crystal. With increase of crystallization temperature for both PA66 and FR-PA66, the endotherm peak shifted slightly to higher temperatures. This phenomenon indicates that TPO unit were embedded into main chain of PA66 and intrinsic flame retardant materials were obtained. The incorporation of TPO has slight effect on the melting temperature of FR-PA66. In addition, by carefully observing the heating curves of FR-PA66, we found that the main endotherm peaks for all samples are broad and have a shoulder peaks near 234°C. We assume that the shoulder peaks were contributed to the melting of para-crystal, which is formed at the second crystallization stage (see § 3.3b). The values of crystallization temperature (T_c) and the main melting temperature (T_m) were obtained directly from figure 2. According to Hoffman–Weeks theory, the equilibrium melting point $\left(T_m^0\right)$ was obtained by linear extrapolation of T_m vs T_c data to intersect the line $T_m = T_c$. It was observed from figure 3 that the values of T_m^0 for FR-PA66 and PA66 are 257·1°C and 265·3°C, respectively. Lower T_m^0 value for FR-PA66 indicate that the crystals in FR-PA66 were not perfect than virgin PA66 (Ma *et al* 2007), and incorporation of TPO is unfavourable for FR-PA66 crystals.

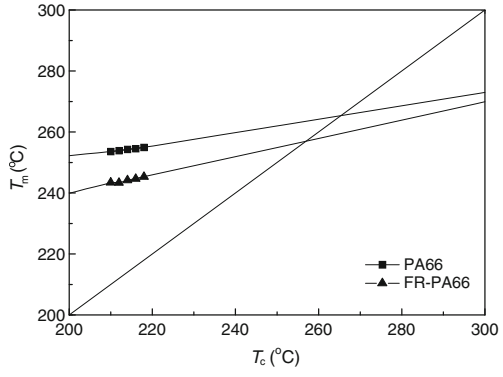

Figure 3. Melting temperature as a function of crystallization temperature for PA66 and FR-PA66.

3.2 *Isothermal crystallization kinetics*

3.2a *DSC curves of isothermal crystallization and crystallinity change curves*: The isothermal crystallization curves of FR-PA66 and PA66 at different T_c are illustrated in figure 4. And the curves of degree of crystallinity vs time, t are presented in figure 5. The crystallization parameters such as half-crystallization time, $t_{1/2}$ and maximum crystallization time, t_{max} were obtained from figure 5 and are listed in table 1. The data show that the half-crystallization time, $t_{1/2}$ and maximum crystallization time, t_{max} of FR-PA66 are prolonged than that of PA66 at the same degree of crystallinity. This is due to the TPO unit that blocks the gathering and rearranging of PA66 macromolecule chains, which result in the difficulty in forming regular hydrogen bond and dislocation of functional groups. Hence the regularity and symmetry of the chain were destroyed to a certain extent, and the crystallization ability and rate of FR-PA66 were declined. In addition, the rigidity of TPO also blocks the movement of chain segment and restricts spreading and arranging of chain segment to crystal nucleus, further result in the decline of crystallization rate (Jin and Hua 2005; Xiaofeng Yang *et al* 2009). The prolonging $t_{1/2}$ and t_{max} of FR-PA66 indicates that the first nucleation site in FR-PA66 was not TPO unit, while polyamide unit is still the first nucleation site. Therefore, the incorporation of TPO groups do not change the nucleation mechanism and nucleation pattern of FR-PA66. On the contrary, with the incorporation of TPO groups, the nucleation rate and crystallization properties of FR-PA66 were declined. Thus TPO groups are unfavourable for FR-PA66 crystallization.

Comparing the data in table 1, we can found that the values of $t_{1/2}$, t_{max} of FR-PA66 decrease rapidly with the decrease in crystallization temperature, and the decline rate was faster than that of PA66 at higher crystallization temperature.

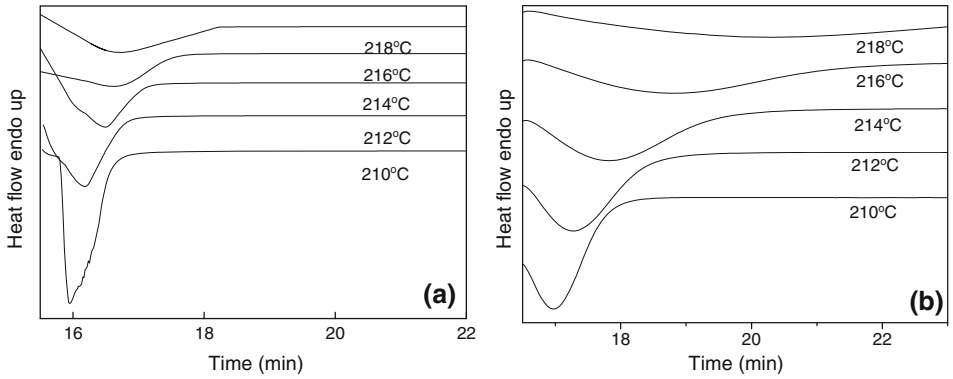

Figure 4. Isothermal crystallization curves of (**a**) PA66 and (**b**) FR-PA66.

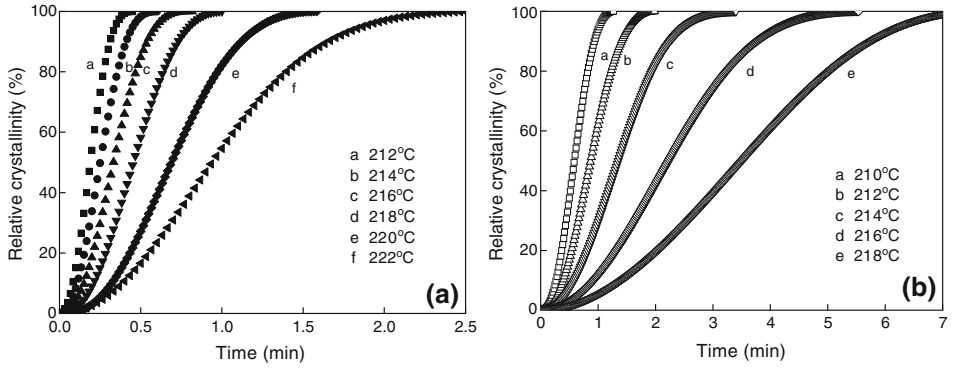

Figure 5. Relative degree of crystallinity of (**a**) PA66 and (**b**) FR-PA66 as a function of time during isothermal crystallization.

Table 1. Values of n, K, t_{max} and $t_{1/2}$ for PA66 and FR-PA66 during isothermal crystallization using Avrami equation.

Sample	T_c (°C)	Avrami index n	K (min^{-1})	$t_{1/2}$ (min)	t_{max} (min)	Correlation coefficient
PA66	210	2·28	34·76	0·18	0·45	0·9972
	212	2·31	18·91	0·25	0·63	0·9978
	214	2·47	11·48	0·33	0·99	0·9983
	216	2·41	5·03	0·45	1·17	0·9965
	218	2·66	1·90	0·68	1·26	0·9983
FR-PA66	210	2·45	2·82	0·58	0·40	0·9971
	212	2·45	1·05	0·87	0·79	0·9983
	214	2·29	0·38	1·35	1·38	0·9980
	216	2·15	0·14	2·22	2·31	0·9972
	218	2·24	0·05	3·48	3·88	0·9965

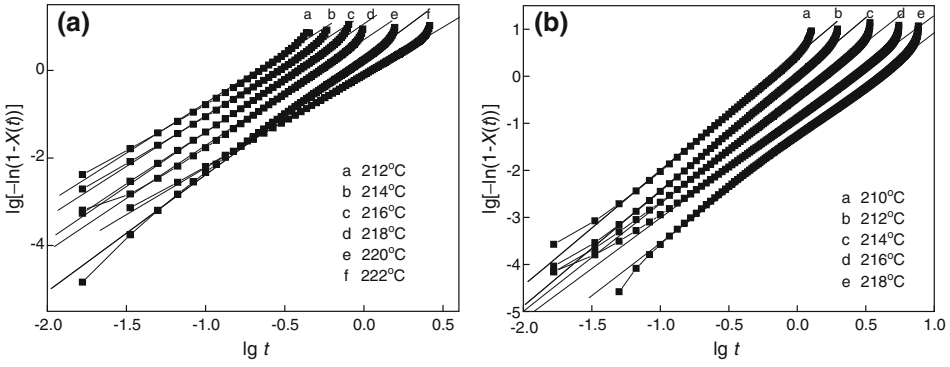

Figure 6. Plot of $\lg[-\ln(1-X(t))]$ vs $\lg t$ for (**a**) PA66 and (**b**) FR-PA66 at various temperatures during isothermal crystallization.

This indicates that the crystallization process of FR-PA66 is controlled by nucleation rate which is similar to PA66. Hence the nucleation ability of polyamide unit in FR-PA66 was strengthened with decline of crystallization temperature. So $t_{1/2}$ and t_{max} of FR-PA66 decreased rapidly.

3.2b *Isothermal crystallization analysis with Avrami equation*: Figure 6 shows the plots of $\lg[-\ln(1-X(t))]$ vs $\lg t$ for FR-PA66 and PA66. The values of Avrami exponent n and crystallization rate K constant were determined from the slope and intercept of the plot, respectively, and are listed in table 1. Better correlation coefficient between $\lg[-\ln(1-X(t))]$ and $\lg t$ values in table 1 indicate that Avrami equation is appropriate for describing the isothermal crystallization kinetics of FR-PA66 and PA66.

Table 1 shows that all the values of n for FR-PA66 and PA66 vary from 2 to 3, further demonstrating that the difference between FR-PA66 and PA66 is unobvious in nucleation mechanism and nucleation pattern. It is seen from table 1 that the K values of FR-PA66 is lower than that of PA66 at the same crystallization temperature. This confirms that TPO unit at first not only unaffects nucleation, but also decreases the nucleation rate of polyamide unit. Hence, the incorporation of TPO declines the crystallization rate of FR-PA66, and is unfavourable for FR-PA66 crystallization.

3.2c *Isothermal crystallization activation energy*: The following equation was obtained from Arrhenius equation:

$$K^{1/n} = A\exp(E_a/RT_c). \quad (4)$$

Here A is the pre-exponential factor, which has nothing to do with temperature; E_a the crystallization activation energy; T_c the absolute crystallization temperature and R the gas constant. By plotting $(1/n)\ln K$ vs $1/T_c$ (see figure 7), the E_a of polymer was obtained and are listed in table 2. Larger E_a values for FR-PA66 further demonstrate that TPO unit is unfavourable for crystallization.

3.3 *Non-isothermal crystallization kinetics*

3.3a *Effects of cooling rate on crystallization*: The non-isothermal crystallization curves of FR-PA66 and PA66

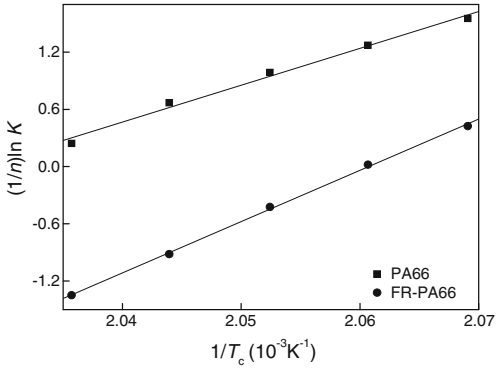

Figure 7. Plot of $(1/n)\ln K$ vs $1/T$ for (**a**) PA66 and (**b**) FR-PA66 during isothermal crystallization.

Table 2. Values of crystallization activation energy for PA66 and FR-PA66.

	Isothermal crystallization		Non-isothermal crystallization	
Sample	Crystallization activation energy E_a (kJ/mol)	Correlation coefficient	Crystallization activation energy E_a (kJ/mol)	Correlation coefficient
PA66	−321·13	0·9957	−336·6	0·9807
FR-PA66	−446·82	0·9995	−432·9	0·9831

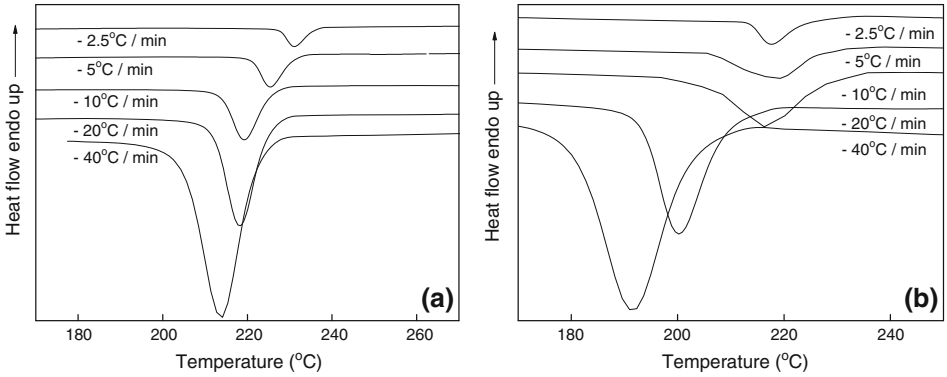

Figure 8. Non-isothermal crystallization curves of (**a**) PA66 and (**b**) FR-PA66.

at various cooling rates are illustrated in figure 8. The crystallization parameters such as crystallization peak temperature (T_p) and time (t_{max}) corresponded to the maximum crystallization rate (t_{max}), the half-crystallization time ($t_{1/2}$) and the crystallization enthalpy (ΔH_c), are listed in table 3. In both the cases, the crystallization peak become broader and T_p shifted to lower temperature with increase in the cooling rate, indicating that the higher the cooling rate, the later crystallization occurred.

The values of t_{max} and $t_{1/2}$ of FR-PA66 were larger than that of PA66, while ΔH_c was smaller at the same cooling rate. As further demonstrated that TPO unit at first does not nucleate during cooling process, which means that the nucleation mechanism and nucleation pattern of FR-PA66 were not changing. On the contrary, TPO groups make the nucleation rate and crystallization rate declining. The result was corresponding with the isothermal crystallization analysis and was further verified by the lower crystallization enthalpy change of FR-PA66 than PA66.

Figure 9 presented the $X_c(T)$ as a function of T for FR-PA66 and PA66. It is seen that all curves had approximately the same reversed sigmoid shapes. As also observed, the higher the cooling rate, the lower the temperature to initiate the crystallization, indicating that there was not enough time to activate nuclei at higher temperatures when crystallized at higher cooling rates. Nucleation, therefore, occurred at lower temperatures. At the same cooling rate, crystallization of FR-PA66 occurred at a lower initial temperature and a broader time range, which indicated that the incorporation of TPO is unfavourable for crystallization and decreased the crystallization rate of FR-PA66.

3.3b *Non-isothermal crystallization analysis with Avrami–Jeziorny equation*: In non-isothermal crystallization, time t has the relation with temperature T as follows

$$t = \frac{|T_0 - T|}{\Phi}, \tag{5}$$

where T_0 and T are the temperatures at initial and time t respectively and Φ is the cooling rate. The values of T on the x-axis in figure 9 can be transformed into crystallization time t according to (5). Figure 10 shows the plots of $\lg[-\ln(1 - X(t))]$ vs $\lg t$ for FR-PA66 and PA66. The values of n and Z_c were determined from the slope and intercept of the plot, respectively, and are listed in table 4. Like other polyamide samples (Ma *et al* 2007), all curves were divided into two sections at the point when the value of $X(t)$ is 90%. And the two sections were named as the primary crystallization stage and the secondary crystallization stage. At the primary stage, the value of n_1 is in the range of 3·4–5·4 for virgin PA66 and 3·6–4·9 for FR-PA66. At the secondary stage, the value of n_2 is in the range of 1·4–3·3 for virgin PA66 and 1·5–1·7 for FR-PA66. It was inferred from these results that free nucleation and growing were the main crystallization processes at the prime crystallization stage, and

Table 3. Values of T_p, t_{max}, ΔH_c and $t_{1/2}$ for PA66 and FR-PA66 during non-isothermal crystallization.

	PA66				FR-PA66			
Φ (°C/min)	T_p (°C)	t_{max} (min)	ΔH_c (J/g)	$t_{1/2}$ (min)	T_p (°C)	t_{max} (min)	ΔH_c (J/g)	$t_{1/2}$ (min)
2·5	231·1	3·0	−69·5	2·6	217·7	6·8	−42·7	6·1
5	225·5	2·0	−72·7	1·8	216·1	4·3	−59·8	4·0
10	219·4	1·3	−75·9	1·2	213·4	2·5	−58·6	2·3
20	218·1	0·9	−90·5	0·8	200·2	1·0	−45·8	0·9
40	214·1	0·5	−97·2	0·04	191·6	0·6	−45·0	0·6

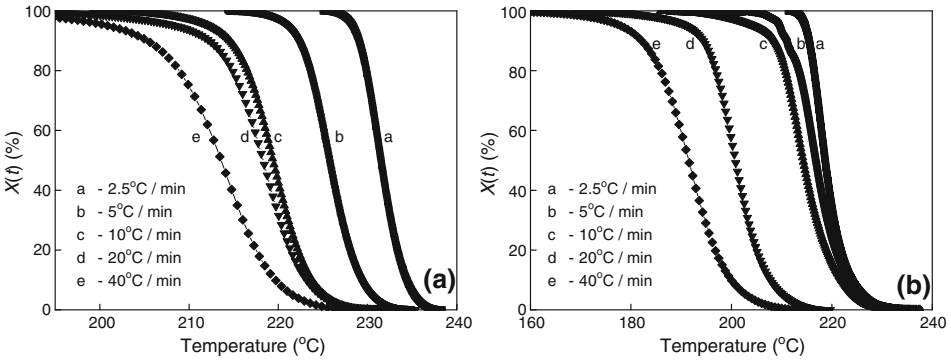

Figure 9. Relative degree of crystallinity of (**a**) PA66 and (**b**) FR-PA66 as a function of temperature at various cooling rates during non-isothermal crystallization.

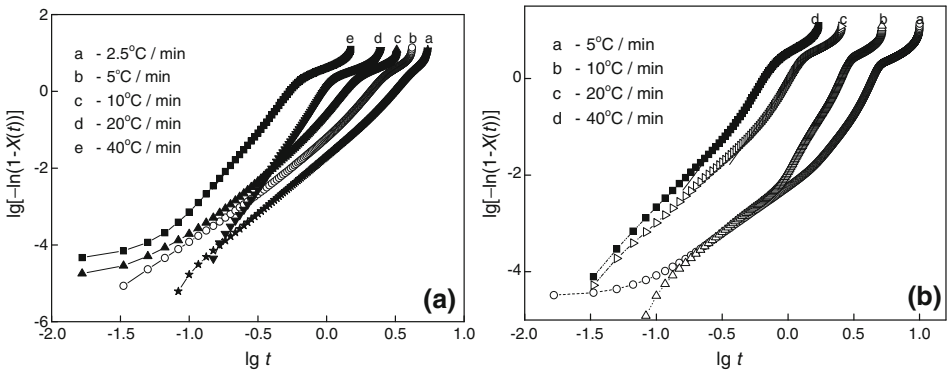

Figure 10. Plot of $\lg[-\ln(1-X(t))]$ vs $\lg t$ for (**a**) PA66 and (**b**) FR-PA66 at various temperatures during non-isothermal crystallization.

Table 4. Values of n_1, Z_{c1}, n_2 and Z_{c2} for PA66 and FR-PA66 during non-isothermal crystallization using Avrami–Jeziorny equation.

	Primary crystallization stage				Secondary crystallization stage			
	PA66		FR-PA66		PA66		FR-PA66	
Φ	n_1	Z_{c1}	n_1	Z_{c1}	n_2	Z_{c2}	n_2	Z_{c2}
2·5	3·44	0·18	–	–	3·35	0·21	–	–
5	3·77	0·30	4·51	0·05	2·30	0·57	1·75	0·38
10	3·98	0·58	4·82	0·14	1·63	1·00	1·67	0·67
20	5·36	1·10	3·81	0·91	1·41	1·33	1·51	1·26
40	4·49	3·28	3·68	1·87	1·52	1·86	1·61	1·70

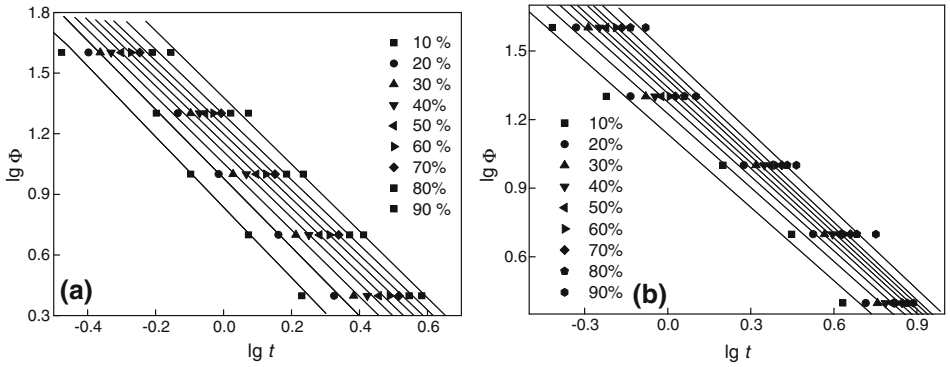

Figure 11. Plot of lg Φ vs lg t for (**a**) PA66 and (**b**) FR-PA66 at various relative degree of crystallinity during non-isothermal crystallization.

Table 5. Values of $F(T)$ and a for PA66 and FR-PA66 at various relative crystallinity obtained from the combined Avrami and Ozawa equations.

Relative degree of crystallinity X (T%)	PA66			FR-PA66		
	$F(T)$	a	R	$F(T)$	a	R
10	6·9	1·75	−0·9889	13·7	1·07	−0·9904
20	9·5	1·70	−0·9931	16·8	1·08	−0·9916
30	11·3	1·65	−0·9939	18·9	1·08	−0·9925
40	12·9	1·63	−0·9953	20·7	1·10	−0·9927
50	14·3	1·61	−0·9970	21·9	1·10	−0·9926
60	15·9	1·61	−0·9975	23·7	1·11	−0·9929
70	17·4	1·60	−0·9979	25·0	1·12	−0·9928
80	19·7	1·61	−0·9984	27·0	1·13	−0·9933
90	24·0	1·65	−0·9982	30·6	1·14	−0·9900

unimensional nucleation and growing were the main crystallization processes at the second crystallization stage. The values of Z_{c1}, Z_{c2} for PA66 are close to that of FR-PA66, which also indicate that the fundamental crystallization mechanism and pattern of FR-PA66 is similar to PA66. But carefully comparing the values, we found that the change in the range of n_1 and n_2 for FR-PA66 is narrower and smaller than that of PA66, and it was especially obvious for n_2. When combining the shoulder peaks in figure 2 for FR-PA66, we think that TPO unit form or help in forming para-crystal accompanying the main-crystal unimensional nucleation and growing during the second crystallization stage, which block or restrict the nucleation and growing direction of main-crystal of FR-PA66 with a certain extent. Therefore, n_2 exhibits a narrow changing range and DSC heating curves show a shoulder peak for FR-PA66.

3.3c *Non-isothermal crystallization analysis with Mo methods*: At the given relative degree of crystallization of PA66 and FR-PA66, the plots of lg Φ vs lg t according to (3) were illustrated in figure 11. Values of a and $F(T)$ were calculated from the slope and intercept of these lines, respectively, and are summarized in table 5. All these plots exhibited a good linear relationship, which indicate that Mo's methods were appropriate for describing non-isothermal crystallization process of FR-PA66.

It can be seen from table 5 that the values of $F(T)$ increased gradually with increasing relative degree of crystallinity, and the $F(T)$ values of FR-PA66 are larger than PA66. As indicated that the crystallization rate of FR-PA66 is lower than that of PA66. That is to say, the crystallization

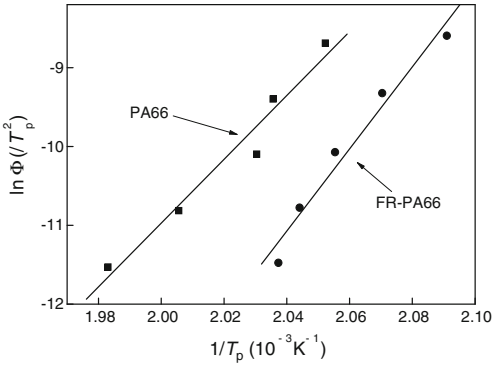

Figure 12. Plot of $\ln\left(\Phi/T_p^2\right)$ vs $1/T_p$ for (**a**) PA66 and (**b**) FR-PA66 during non-isothermal crystallization with Kissinger method.

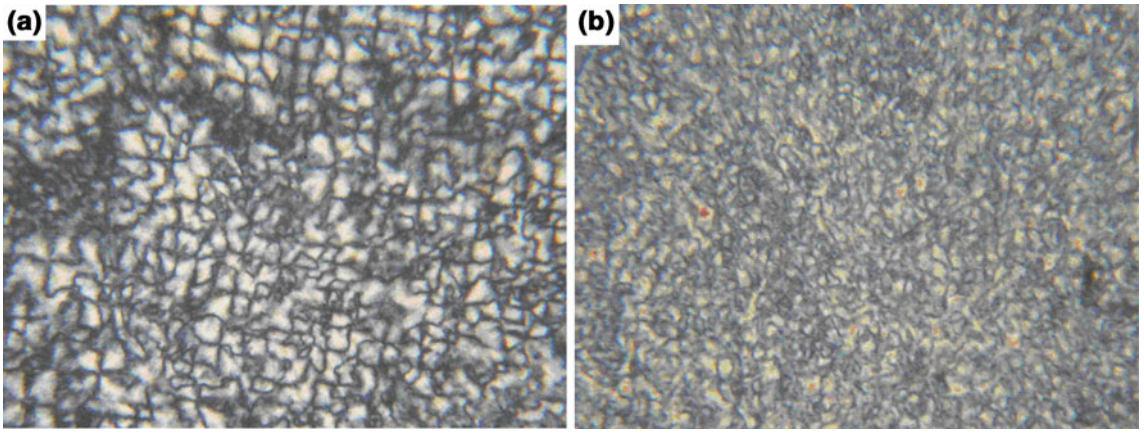

Figure 13. Polarized optical microscopy images for (**a**) PA66 and (**b**) FR-PA66 after constant temperature crystallization 4·5 h at 240°C.

ability of FR-PA66 was declining with TPO unit incorporation. From table 5, we can also found that the values of a of FR-PA66 hold a constant, which further indicates that the fundamental crystallization mechanism and pattern are of no change for FR-PA66.

3.3d *Non-isothermal crystallization activation energy*: Considering the effects of cooling rate on non-isothermal crystallization, Kissinger (1957) given an approach for calculating the activation energy of polymer in non-isothermal crystallization and shown as follows:

$$\frac{d(\ln \Phi/T_p^2)}{d(1/T_p)} = -\frac{\Delta E_a}{R}. \tag{6}$$

The plots of $\ln\left(\Phi/T_p^2\right)$ vs $1/T_p$ were illustrated in figure 12, the values of ΔE_a were calculated from the slope of these lines and are listed in table 2. Similarly with isothermal crystallization, the value of E_a for FR-PA66 is larger than PA66, which further demonstrates that TPO unit restrict the movement of molecule chain of PA66 and make the activation energy of molecule chain movement increasing.

3.4 *POM analysis*

The POM images of FR-PA66 and PA66 are presented in figure 13. It is observed from figure 13 that both FR-PA66 and PA66 exhibit right-angled intersection extinction phenomenon and spherulite was formed. Above phenomenon indicate that the incorporation of TPO groups do not change the nucleation mechanism and nucleation pattern of FR-PA66. But comparing with PA66, the spherulite dimensions of FR-PA66 reduce obviously and the boundary of spherulite is indistinct. This indicates that TPO groups are unfavorable for FR-PA66 crystallization. The results are according to isothermal crystallization and non-isothermal crystallization analyses. In addition, it is seen from figure 13 that the crystallization region of FR-PA66 is less than PA66 and the spherulite defect of FR-PA66 is more than that of PA66.

4. Conclusions

A series of researches such as isothermal crystallization behaviour, non-isothermal crystallization behaviour and POM image of FR-PA66 indicate that TPO unit does not nucleate at first during crystallization process of FR-PA66. The nucleation mechanism and nucleation pattern of FR-PA66 do not virtually change with incorporation of TPO groups. The main crystallization process of FR-PA66 is free nucleation and growing during the prime crystallization stage, and is unimensional nucleation and growing during the second crystallization stage. But at the second crystallization stage, we think there is a para-crystal forming with the main-crystal unimensional nucleation and growing. In addition, incorporation of TPO groups result in the decrement of both nucleation rate and crystallization rate of FR-PA66, and the increase of crystallization activation energy. Hence TPO groups are unfavourable for FR-PA66 crystallization. In addition, introducing of TPO groups also result in the decrease in the crystallization region of FR-PA66 and increase in spherulite defect.

Acknowledgements

The work was supported by Natural Science Foundation of Shanxi (Grant No. 2010021022-3) and the Scientific Research Foundation of the Higher Education Institutions of Shanxi Province, China (Grant No. 2010115).

References

Avrami M 1939 *J. Chem. Phys.* **7** 1103
Avrami M 1940 *J. Chem. Phys.* **8** 212

Avrami M 1941 *J. Chem. Phys.* **9** 177
Gao Huan and Mo Zhishen 1992 *Acta Polym. Sin.* **2** 162
Jeziorny A 1978 *Polymer* **19** 1142
Jin Y G and Hua Y Q 2005 *Polymer physics* (Chemical Industry Press: Beijing) vol. 29 114
Kissinger H E 1957 *Anal. Chem.* **29** 1702
Liu Jieping and Mo Zhishen 1991 *Polym. Bull.* **4** 9
Liu T X, Mo Z S, Wang G and Zhang H F 1997 *Polym. Eng. Sci.* **37** 568
Ma Y L, Hu G S, Ren X L and Wang B B 2007 *Mater. Sci. Eng. A* **460–461** 611
Ozawa T 1971 *Polymer* **12** 150
Xiaofeng Yang, Qiaoling Li, Zhiping Chen and Hongli Han 2009 *Bull. Mater. Sci.* **32** 375